Chem. Pharm. Bull.

Regular article

Dibutyltin(IV) Complexes Derived from L-DOPA: Synthesis, Molecular Docking, Cytotoxic and Antifungal Activity

Running title: Organotin(IV) complexes cytotoxic and antifungal agents

Erika Rocha-del Castillo[a], Omar Gómez-García[b], Dulce Andrade-Pavón[c], Lourdes Villa-Tanaca[c], Teresa Ramírez-Apan[a], Antonio Nieto-Camacho[a] and Elizabeth Gómez[a]*

[a]*Instituto de Química, Universidad Nacional Autónoma de México (UNAM), Circuito Exterior s/n, Ciudad Universitaria, 04510 Ciudad de México, México:* [b]*Departamento de Química Orgánica-Laboratorio de Síntesis de Fármacos Heterocíclicos, Escuela Nacional de Ciencias Biológicas-Instituto Politécnico Nacional, Prolongación de Carpio y Plan de Ayala S/N, Colonia Santo Tomás, 11340, Ciudad de México, México;* [c]*Departamento de Microbiología-Laboratorio de Biología Molecular de Bacterias y Levaduras, Escuela Nacional de Ciencias Biológicas-Iinstituto Politécnico Nacional, Prolongación de Carpio y Plan de Ayala S/N, Colonia Santo Tomás, 11340, Ciudad de México, México.*

**Corresponding author. Email: eligom@iquimica.unam.mx*

Key words: Organotin(IV), Cytotoxicity, Antifungal, Toxicity, Molecular docking, Multinuclear NMR

Abstract

A series of organotin(IV) complexes was herein prepared and characterized. A one-pot synthetic strategy afforded reasonable to high yields, depending on the nature of the ligand. All new complexes were fully characterized by spectroscopic techniques, consisting of IR, MS and NMR (^{1}H, ^{13}C and ^{119}Sn). The *in vitro* cytotoxicity tests demonstrated that the organotin complexes produced a greater inhibition, versus *cis*platin (the positive control), of the growth of six human cancer cell lines: U-251 (glioblastoma), K-562 (chronic myelogenous leukemia), HCT-15 (colorectal), MCF-7 (breast), MDA-MB-231 (breast) and SKLU-1 (non-small cell lung). The potency of this cytotoxic activity depended on the nature of the substituent bonded to the aromatic ring. All complexes exhibited excellent IC_{50} values. The test compounds were also screened *in vitro* for their antifungal effect against *Candida glabrata* and *Candida albicans*, showing MIC (minimum inhibitory concentration) values lower than those obtained for fluconazole. A brine shrimp bioassay was performed to examine the toxic properties. Molecular docking studies demonstrated that the organotin(IV) complexes bind at the active site of topoisomerase I in a similar manner to topotecan, sharing affinity for certain amino acid side chains (Ile535, Arg364 and Asp533), as well as for similar DNA regions (DA113, DC112 and DT10).

1. INTRODUCTION

Schiff bases are useful ligands and important organic fragments. The azomethine (C=N) functional group is a versatile pharmacophore for the design of bioactive compounds with a broad range of effects, including anti-inflammatory [1, 2], antibacterial [3, 4], antifungal [3], analgesic [2, 5], antimicrobial [3, 6, 7], anticonvulsant [5], antitubercular, anticancer [5, 8], antioxidant [9], anthelmintic [10], antiglycation [11] and antidepressant [12].

Schiff bases are extensively employed as chelating ligands in the field of coordination chemistry. The metallic complexes of these compounds have been widely studied due to their structural diversity, physical and chemical properties, and pharmacological activities. What makes metal-based compounds particularly interesting are the properties that can be modified to improve the therapeutic effect, especially the ligand exchange rate, coordination affinity, variability of the oxidation state, bioavailability and biodistribution.

Among Schiff bases, the organotin (IV) complexes containing NS, NO, ONO and ONS donor atoms have shown great appeal due to their structural features, which can provide antimicrobial, antifungal, antibacterial, antioxidant and carcinostatic activity [9, 13-16]. The amino acids and their derivatives have been the subject of intense research efforts because of their coordination properties and potential for generating effective and less toxic metal-based drugs. Additionally, their physico-chemical properties and specific mechanism of transport facilitate facile biological uptake [17].

L-3,4-dihydroxyphenylalanine (L-DOPA) is a bioactive amino acid that produces dopamine in the body after oral ingestion. Commonly administered for symptom management in patients with Parkinson's disease (PD), it is always accompanied by a peripheral DOPA decarboxylase inhibitor (*e.g.*, carbidopa) to reduce its rapid conversion into dopamine in peripheral tissues [18]. L-DOPA derivatives may have promise for other pharmacological effects, evidenced by the fact that various amino acids used as building blocks to generate Schiff base ligands and their organotin (IV) complexes have demonstrated antiproliferative, antibacterial and antimicrobial activity [19-24]. Indeed, the biological activity of these compounds is generally enhanced by carefully choosing the organic ligands associated with the metal [25]. Therefore, it is essential to understand the properties of both the ligands and metal for the synthesis of biologically active compounds.

The urgency for the development of new antifungal agents has increased in the last few years as a result of the greater incidence in hospitals of *Candida* infections, especially *C. albicans* and *C. glabrata* [26, 27]. Although new drugs have been introduced to combat fungal diseases, resistance to such agents has been outpacing development, particularly in patients who require long term-treatment. Hence, it is necessary to seek alternatives for treating patients with diseases provoked by *Candida* species [28].

We have undertaken the one-pot synthesis of new organotin (IV) complexes derived from L-3,4-dihydroxyphenylalanine Schiff bases as donor ligands. In the present study, a series of pentacoordinated diorganotin (IV) complexes were prepared and then characterized by means of ultraviolet-visible (UV-Vis), infrared (IR), and ^{1}H, ^{13}C and ^{119}Sn NMR spectrometry, as well as mass spectrometry (MS). The complexes were tested on six human cancer cell lines and their toxicity was evaluated using the brine shrimp lethality assay. Finally, they were screened *in vitro* for antifungal activity against *Candida glabrata* and *Candida albicans*.

2. MATERIALS AND METHODS

2.1 Materials

All reagents and solvents were obtained from Sigma-Aldrich and used without further purification.

2.2 Physical measurements

The melting points of the complexes were measured with a Fischer-Johns MEL-TEMP II apparatus and are uncorrected. The infrared (IR) spectra of the ligands and complexes were recorded on a BRUKER TENSOR 27 spectrometer utilizing KBr. Molar conductivity measurements were recorded by using a Hanna HI9033 apparatus with anhydrous methanol as solvent. The UV-Vis absorption spectra were obtained on a Cary 50 Varian spectrometer in methanol at 2.0435 μM for all complexes. ^{1}H, ^{13}C and ^{119}Sn spectra were recorded with a Bruker Advance III spectrometer at 300.0, 75.4 and 111.8 MHz, respectively, in chloroform-*d* or DMSO-d_6. The ^{1}H and ^{13}C signals were completely assigned by means of COSY, HSQC and HMBC experiments. The FAB (fast atom bombardment) mass spectra were recorded on

a JEOL-JMS-X103 spectrometer, and poly(ethylene glycol) 600 served as the matrix for precise mass spectra.

2.3 General procedure for the synthesis of complexes 3a-3h

To a solution of 0.803 mmol of 3,4-dihydroxi-L-phenylalanine (L-DOPA) in 20 mL of methanol, 0.803 mmol of the corresponding 5-R-salicylaldehyde (R= H, CH_3, OH, OCH_3, Cl, Br, I, NO_2) were added. After the reaction mixture was refluxed for 30 min, dibutyltin oxide was added in a stoichiometric ratio and the reaction was refluxed for another 8 h under constant stirring. Subsequently, the reaction mixture was filtered and the solvent removed under reduced pressure to afford the resulting compound as a solid. All compounds were purified by crystallization from methanol and have an intense bright yellow or orange color. The majority of the compounds are soluble in most common organic solvents.

(5*S*)-2,2-Di-*n*-butyl-6-aza-1,3-dioxa-5-(3',4'-dihydroxybenzyl)-12-methoxy-2-stannabenzocyclodonone-6,8-dien-4-one **(3a)**

The general procedure with 0.1 mL (0.803 mmol) 5-methoxysalicylaldehyde gave compound **3a** as an orange powder in 78% yield (0.3514g); m.p. 112-115 °C; $[\alpha]\ ^{20}_D$= -26.6 (C=1, Methanol). Molar conductance Λ_M (1×10^{-3} M, Methanol): 8.0 $ohm^{-1}\ cm^2\ mol^{-1}$ (non-electrolyte). UV-Vis (Methanol) [λ_{max}/nm ($\log\varepsilon$/mol $L^{-1})^{-1}\ cm^{-1}$]: 205 (30125), π–π* (aromatic), 290 (6408), π–π* (C=N), 425 (2232) n–π*(C=N); IR (KBr, cm^{-1}): 3061 ν(OH $_{alcohol}$), 1652 ν_{asym} (COO^-), 1598 ν(C=N), 1359 ν_{sym}(COO^-), 1257ν_{arom}(CO), 572 ν(Sn-C), 549 ν(Sn-O), 452 ν(Sn-N). ^{1}H NMR (300.52 MHz, DMSO-*d6*) δ: 8.83 (s,1H, OH), 8.76 (s,1H, OH), 8.36 (s, $^3J^1H$-^{119}Sn = 51.1 Hz, 1H, H-7), 7.08 (dd, *J* = 9.1, 3.2 Hz, 1H, H-10), 6.74 (d, *J* = 3.3 Hz, 1H, H-13), 6.62 (d, *J* = 9.1 Hz, 1H, H-11), 6.56 (d, *J* = 8.0 Hz, 1H, H-6'), 6.50 (d, *J* = 2.0 Hz, 1H, H-2'), 6.26 (dd, *J* = 8.0, 2.0 Hz, 1H, H-5'), 4.28 (t, *J* = 5.1 Hz, 1H, H-5), 3.68 (s, 3H, H-16), 3.04 (dd, *J* = 12.0, 6.0 Hz, 2H, H-14), 1.59-0.88 (m, 12H, H-α, β, γ, α', β', γ'), 0.84 (t, *J* = 6.0 Hz, 3H, H-δ), 0.74 (t, *J* = 6.0 Hz, 3H, H-δ'). ^{13}C NMR (75.57 MHz, DMSO-d_6) δ: 173.9 (C-9), 172.5 (C-4), 163.5 (C-7), 149.6 (C-12), 145.3 (C-3'), 144.4 (C-4'), 126.4 (C-10), 125.9 (C-1'), 122.7 (C-11), 120.8 (C-5'), 117.2 (C-2'), 116.3 (C-8), 116.0 (C-13), 115.4 (C-6'), 67.7 (C-5), 55.5 (C-16), 40.4 (C-14), 26.7, 26.6 (C-α, C-α'), 26.0, 25.9 (C-β, C-β'), 21.5, 21.4 (C-γ, C-γ'), 13.6,13.5 (C-δ, C-δ'). ^{119}Sn NMR (112.07 MHz, DMSO-

d6) δ: -216.77. ^{119}Sn NMR (112.07 MHz, chloroform-*d*) δ: -192.5. FAB-MS m/z (%): [(M^++1), 564] (5), [M^+- CO_2, 520] (13), [M^+-2Bu, 444] (8), [M^+- $CHC_6H_3(OH)_2$, 441] (3), [M^+-C_3H_7, 520] (12), [M^+-Bu-OCH_3-$CH_2C_6H_3(OH)_2$, 355] (100). HR-MS (FAB^+) m/z: 564.1408 (calcd for $C_{25}H_{34}NO_6Sn$); observed: 564.1413.

(5*S*)-2,2-Di-*n*-butyl-6-aza-1,3-dioxa-5-(3',4'-dihydroxybenzyl)-12-hydroxy-2-stannabenzocyclodonone-6,8-dien-4-one (**3b**)

The general procedure with 0.1109 g (0.803 mmol) 5-hydroxysalicylaldehyde furnished compound **3b** as an orange powder in 84% yield (0.3670g); m.p.$_{dec}$ 209 °C. [α] $^{20}_D$= -230 (C=1, Methanol). Molar conductance Λ_M (1×10^{-3} M, Methanol): 7.0 ohm^{-1} cm^2 mol^{-1} (non-electrolyte). UV-Vis (methanol) [λ_{max}/nm ($\log\varepsilon$/mol $L^{-1})^{-1}$ cm^{-1}]: 205 (57045), π–π* (aromatic), 290 (14596), π–π* (C=N), 430 (4824), n–π* (C=N); IR (KBr, cm^{-1}): 3153 ν(OH $_{alcohol}$), 1628 ν_{asym} (COO^-), 1606 ν(C=N), 1375 ν_{sym}(COO^-), 1259 ν_{arom}(CO), 1258 ν(C-O $_{arom}$) 586 ν(Sn-C), 510 ν(Sn-O), 445 ν(Sn-N). ^{1}H NMR (300.52 MHz, DMSO-*d6*) δ: 8.92 (s,1H, OH), 8.82 (s,1H, OH), 8.74 (s,1H, OH), 8.21 (s, $^3J^1H$-^{119}Sn = 51.1 Hz, 1H, H-7), 6.92 (dd, *J* = 9.0, 3.0 Hz, 1H, H-10), 6.58-6.49 (m, 4H, H-6', H-13, H-11, H-2'), 6.26 (dd, *J* = 9.0, 3.0 Hz, 1H, H-5'), 4.26 (t, *J* = 5.4 Hz, 1H, H-5), 3.01 (dd, *J* = 13.8, 5.6 Hz, 2H, H-14), 1.51-1.08 (m, 12H, H-α, β, γ, α', β', γ'), 0.85 (t, *J* = 6.0 Hz, 3H, H-δ), 0.74 (t, *J* = 6.0 Hz, 3H, H-δ'). ^{13}C NMR (75.57 MHz, DMSO-*d6*) δ: 173.7 (C-9), 172.5 (C-4), 162.1 (C-7), 147.3 (C-12), 145.3 (C-3'), 144.4 (C-4'), 126.8 (C-10), 126.0 (C-1'), 122.9 (C-11), 120.8 (C-5'), 118.1 (C-13), 117.1 (C-2'), 116.5 (C-8), 115.3 (C-6'), 67.7 (C-5), 39.9 (C-14), 26.7, 26.6 (C-α, C-α'), 26.0, 25.8 (C-β, C-β'), 21.2 (C-γ, C-γ'), 13.6, 13.4 (C-δ, C-δ'); ^{119}Sn NMR (112.07 MHz, DMSO-*d6*) δ: -214.0. ^{119}Sn NMR (112.07 MHz, chloroform-*d*) δ: -193.4. FAB-MS m/z (%): [(M^++1), 550] (6), [M^+- CO_2, 506] (11), [M^+-2Bu, 435] (3), [M^+- $CHC_6H_3(OH)_2$-H_2O, 410] (13), [M^+-C_3H_7, 506] (11), [M^+-Bu-OH-$CH_2C_6H_3(OH)_2$, 355] (100); HR-MS (FAB^+) m/z: 550.1252 (calcd for $C_{24}H_{32}NO_6Sn$); observed: 550.1253.

(5*S*)-2,2-Di-*n*-butyl-6-aza-1,3-dioxa-5-(3',4'-dihydroxybenzyl)-12-methyl-2-stannabenzocyclodonone-6,8-dien-4-one (**3c**)

The general procedure with 0.1109 g (0.803 mmol) 5-methylsalicylaldehyde provided compound **3c** as a yellow powder in 56% yield (0.2445g); m.p. 115-120°C; [α] $^{20}_D$= -26.6

(C=1, Methanol). Molar conductance Λ_M (1×10^{-3} M, methanol): 6.0 ohm^{-1} cm^2 mol^{-1} (non-electrolyte). UV-Vis (methanol) [λ_{max}/nm (logε/mol $L^{-1})^{-1}$ cm^{-1}]: 205 (54006), π–π* (aromatic), 285 (15215), π–π* (C=N), 400 (4745), n–π* (C=N). IR (KBr, cm^{-1}): 3148 ν(OH $_{alcohol}$), 1621 ν_{asym} (COO^-), 1598 ν(C=N), 1374 ν_{sym}(COO^-), 1258 ν_{arom}(C-O), 578 ν(Sn-C), 509 ν(Sn-O), 447 ν(Sn-N). ^{1}H NMR (300.52 MHz, DMSO-*d*$_6$) δ: 8.83 (s,1H, OH), 8.75 (s,1H, OH), 8.32 (s, $^3J^1H$-^{119}Sn = 51.1 Hz, 1H, H-7), 7.22 (dd, *J* = 8.6, 2.4 Hz, 1H, H-10), 6.98 (d, *J* = 2.4 Hz, 1H, H-13), 6.59 (d, *J* = 8.5 Hz, 1H, H-11), 6.59 (d, *J* = 8.5 Hz, 1H, H-11), 6.51 (d, *J* = 2.1 Hz, 1H, H-2'), 6.26 (dd, *J* = 8.0, 2.1 Hz, 1H, H-5'), 4.29 (t, *J* = 5.5 Hz, 1H, H-5), 3.03 (dd, *J* = 13.8, 5.7 Hz, 2H, H-14), 2.18 (s, 3H, H-15), 1.61-0.91 (m, 12H, H-α, β, γ, α', β', γ'), 0.84 (t, *J* = 6.0 Hz, 3H, H-δ), 0.74 (t, *J* = 6.0 Hz, 3H, H-δ'). ^{13}C NMR (75.57 MHz, DMSO-*d*$_6$) δ: 174.0 (C-9), 172.5 (C-4), 166.6 (C-7), 145.3 (C-3'), 144.4 (C-4'), 138.4 (C-10), 135.0 (C-13), 125.9 (C-1'), 124.8 (C-12), 121.6 (C-11), 120.8 (C-5'), 117.1 (C-8), 116.9 (C-2), 115.4 (C-6'), 67.7 (C-5), 39.8 (C-14), 26.7, 26.6, (C-α, C-α'), 26.0, 25.8 (C-β, C-β'), 21.5, 21.4 (C-γ, C-γ'), 19.6 (C-15) 13.6,13.45 (C-δ, C-δ'); ^{119}Sn NMR (112.07 MHz, DMSO-*d*$_6$) δ: -218.0; ^{119}Sn NMR (112.07 MHz, chloroform-*d*) δ: -193.9. FAB-MS m/z (%): [(M^++1), 546] (5), [M^+- CO_2, 504] (10), [M^+-2Bu-H_2O, 414] (18), [M^+-$C_2H_4C_6H_3(OH)_2$, 411] (15), [M^+- $C_2H_4C_6H_3(OH)_2$-CO_2, 368] (10), [M^+-2Bu-CO_2-$(OH)_2$, 355] (100). HR-MS (FAB^+) M/Z: 548.1459 (calcd for $C_{25}H_{34}NO_5Sn$); observed: 548.1470.

(5*S*)-2,2-Di-*n*-butyl-6-aza-1,3-dioxa-5-(3',4'-dihydroxybenzyl)-2-stannabenzocyclodonone-6,8-dien-4-one **(3d)**

The general procedure with 0.1109 g (0.803 mmol) salicylaldehyde delivered compound **3d** as a yellow powder in 65% yield (0.2760g); m.p.$_{dec}$ 210 °C. [α] $^{20}_D$= -140.3 (C=1, Methanol). Molar conductance Λ_M (1×10^{-3} M, Methanol): 5.0 ohm^{-1} cm^2 mol^{-1} (non-electrolyte). UV-Vis (Methanol) [λ_{max}/nm (logε/mol $L^{-1})^{-1}$ cm^{-1}]: 205 (50801), π–π* (aromatic), 285 (12665), π–π* (C=N), 390 (3455), n–π* (C=N). IR (KBr, cm^{-1}): 3050 ν($OH_{alcohol}$), 1647 ν_{asym} (COO^-), 1609 ν(C=N), 1345 ν_{sym}(COO^-), 1252 ν_{arom}(C-O), 552 ν(Sn-C), 503 ν(Sn-O), 444 ν(Sn-N). ^{1}H NMR (300.52 MHz, DMSO-*d*$_6$) δ: 8.84 (s,1H, OH), 8.75 (s,1H, OH), 8.36 (s, $^3J^1H$-^{119}Sn = 48.1 Hz, 1H, H-7), 7.66 (dd, *J* = 7.7, 1.8 Hz, 1H, H-10), 7.51 (td, *J* = 7.7, 1.8, 1H, H-11), 7.39 (td, *J* = 7.75, 1.53, Hz, 1H, H-12), 7.19 (dd, *J* = 7.9, 1.8 Hz, 1H, H-13), 6.56 (d, *J* = 8.0 Hz, 1H, H-6'), 6.51 (d, *J* = 2.0 Hz, 1H, H-2'), 6.26 (dd, *J* = 8.0, 2.1 Hz, 1H, H-5'),

4.31 (t, *J* = 5.4, 1H, H-5), 3.04 (dd, *J* = 13.7, 5.5 Hz, 2H, H-14), 1.59-0.89 (m, 12H, H-α, β, γ, α', β', γ'), 0.84 (t, *J* = 6.0 Hz, 3H, H-δ), 0.73 (t, *J* = 6.0 Hz, 3H, H-δ'). ^{13}C NMR (75.57 MHz, DMSO-*d*$_6$) δ: 174.3 (C-9), 172.5 (C-4), 168.4 (C-7), 145.3 (C-3'), 144.4 (C-4'), 137.0 (C-10), 136.4 (C-13), 125.9 (C-1'), 121.7 (C-11), 120.8 (C-5'), 117.5 (C-8), 117.2 (C-12), 116.4 (C-2'), 67.7 (C-5), 40.4 (C-14), 26.7, 26.6 (C-α, C-α'), 26.0, 25.8 (C-β, C-β'), 21.8, 21.6 (C-γ, C-γ'), 13.6, 13.4 (C-δ, C-δ'). ^{119}Sn NMR (112.07 MHz, DMSO-*d*$_6$) δ: -221.34; ; ^{119}Sn NMR (112.07 MHz, chloroform-*d*) δ: -194.60; FAB-MS m/z (%): [(M^++1), 534] (5), [M^+- CO_2, 490] (22), [M^+-Bu-2H_2O, 440] (8), [M^+- $C_2H_4C_6H_3(OH)_2$, 411] (15), [M^+-$C_2H_4C_6H_3(OH)_2$-CO_2, 353] (40), [M^+-2Bu, 418] (15); HR-MS (FAB$^+$) m/z: 534.1302 (calcd for $C_{24}H_{32}NO_5Sn$); observed: 534.1302.

(5*S*)-2,2-Di-*n*-butyl-6-aza-1,3-dioxa-5-(3',4'-dihydroxybenzyl)-12-Iodo-2-stannabenzocyclodonone-6,8-dien-4-one (**3e**)

The general procedure with 0.1109 g (0.803 mmol) 5-Iodosalicylaldehyde produced compound **3e** as a yellow powder in 82% yield (0.4348g); m.p.$_{dec}$ 175 °C; [α] $^{20}_D$= -26.6 (C=1, Methanol. Molar conductance Λ_M (1×10^{-3} M, Methanol): 4.0 ohm^{-1} cm^2 mol^{-1} (non-electrolyte). UV-Vis (Methanol) [λ_{max}/nm (logε/mol L^{-1})$^{-1}$ cm^{-1}]: 205 (60223), π–π* (aromatic), 280 (4734), π–π* (C=N), 390 (1305) n–π* (C=N). IR (KBr, cm^{-1}): 2955 ν(OH $_{alcohol}$), 1645 ν_{asym} (COO^-),1607 ν(C=N), 1375 ν_{sym}(COO^-), 1258 ν_{arom}(C-O), 561 ν(Sn-C), 535 ν(Sn-O), 444 ν(Sn-N). ^{1}H NMR (300.52 MHz, DMSO-*d*$_6$) δ: 8.83 (s,1H, OH), 8.77 (s,1H, OH), 8.39 (s, $^3J^1H$-^{119}Sn = 45.08 Hz, 1H, H-7), 7.59 (d, *J* = 7.9 Hz, 2H, H-10, H-13), 6.56 (d, *J* = 8.0 Hz, 1H, H-6'), 6.50 (d, *J* = 3.0 Hz, 1H, H-5'), 6.52 – 6.47 (m, 2H, H-11,H-2'), 6.26 (dd, *J* = 8.1, 1.8 Hz, 1H, H-5'), 4.28 (t, *J* = 6.0, 1H, H-5), 3.06 (dd, *J*=13.5, 6.0 Hz, 2H, H-14), 1.58-0.87 (m, 12H, H-α, β, γ, α', β', γ'), 0.82 (t, *J* = 7.1 Hz, 3H, H-δ), 0.74 (t, *J* = 7.2 Hz, 3H, H-δ'). ^{13}C NMR (75.57 MHz, DMSO-*d*$_6$) δ: 173.4 (C-9), 172.3 (C-4), 167.9 (C-7), 145.3 (C-3'), 144.4 (C-4'), 144.3 (C-10), 143.4 (C-13),125.8 (C-1'),124.5 (C-11), 120.8 (C5'), 120.0 (C-8), 117.1 (C-2'), 115.4 (C-6'), 67.8 (C-5), 40.2 (C-14), 26.7, 26.6 (C-α, C-α'), 25.9, 25.8 (C-β, C-β'), 22.4, 22.1 (C-γ, C-γ'), 13.6, 13.4 (C-δ, C-δ'). ^{119}Sn NMR (112.07 MHz, DMSO-*d*$_6$) δ: -227.77. ^{119}Sn NMR (112.07 MHz, Chloroform-*d*) δ: -194.08; FAB-MS m/z (%): [(M^++1), 660] (5), [M^+- CO_2, 616] (20), [M^+-2Bu, 544] (8), [M^+-2Bu-

CO_2, 498] (12), [M^+- $CH_2C_6H_3(OH)_2$-I, 412] (23), [M^+-$C_2H_4C_6H_3(OH)_2$-CO_2-I, 355] (100); HR-MS (FAB^+) M/Z: 660.0269 (calcd for $C_{24}H_{31}NO_5SnI$); observed: 660.0261.

(5*S*)-2,2-Di-*n*-butyl-6-aza-1,3-dioxa-5-(3',4'-dihydroxybenzyl)-12-bromo-2-stannabenzocyclodonone-6,8-dien-4-one (**3f**)

The general procedure with 0.1109 g (0.803 mmol) 5-Bromosalicylaldehyde generated compound **3f** as a yellow powder in 62% yield (0.3018 g); m.p.$_{dec}$ 210 °C. [α] $^{20}_D$= -122 (C=1, Methanol). Molar conductance Λ_M (1×10^{-3} M, Methanol): 9.0 ohm^{-1} cm^2 mol^{-1} (non-electrolyte). UV-Vis (Methanol) [λ_{max}/nm (logε/mol $L^{-1})^{-1}$ cm^{-1}]: 205 (58265), π–π* (aromatic), 285 (10884), π–π* (C=N), 400 (4118) n–π* (C=N). IR (KBr, cm^{-1}): 2955 ν(OH $_{alcohol}$), 1649 ν_{asym} (COO^-), 1612 ν(C=N), 1354 ν_{sym}(COO^-), 1259 ν_{arom}(C-O), 569 ν(Sn-C), 531 ν(Sn-O), 446 ν(Sn-N). ^{1}H NMR (300.52 MHz, DMSO-*d*$_6$) δ: 8.84 (s,1H, OH), 8.77 (s,1H, OH), 8.38 (s, $^3J^1H$-^{119}Sn = 48.09 Hz, 1H, H-7), 7.47 (dd, *J* = 8.9, 2.2 Hz, 1H, H-10), 7.43, (d, *J* = 2.2 Hz, H-13), 6.62 (d, *J* = 8.9 Hz, 1H, H-11), 6.56 (d, *J* = 8.0 Hz, 1H, H-6'), 6.49 (s, 1H, H-2'), 6.26 (d, *J* = 8.1, 1H, H-5'), 4.28 (t, *J* = 5.1 Hz, 1H, H-5), 3.05 (dd, *J* = 13.9, 5.3 Hz, 2H, H-14), 1.69-1.04 (m, 12H, H-α, β, γ, α', β', γ'), 0.83 (t, *J* = 6.0 Hz, 3H, H-δ), 0.74 (t, *J* = 6.0 Hz, 3H, H-δ'). ^{13}C NMR (75.57 MHz, DMSO-*d*$_6$) δ: 173.1 (C-9), 172.1 (C-4), 167.2 (C-7), 145.1 (C-3'), 144.2 (C-4'), 138.7 (C-10), 136.9 (C-13), 125.5 (C-1'), 123.9 (C-11), 120.5 (C-5'), 118.7 (C-8), 116.9 (C-2'), 115.1 (C-6'), 105.9 (C-12), 67.7 (C-5), 40.4 (C-14), 26.4, 26.3 (C-α, C-α'), 25.7, 25.6 (C-β, C-β'), 22.2, 22.0 (C-γ, C-γ'), 13.3, 13.2 (C-δ, C-δ'). ^{119}Sn NMR (112.07 MHz, DMSO-*d*$_6$) δ: -229.92; ^{119}Sn NMR (112.07 MHz, Chloroform-*d*) δ: -194.9. FAB-MS m/z (%): [(M^++1), 612] (17), [M^+- CO_2, 668] (24), [M^+-2Bu, 496] (17), [M^+-2Bu-CO_2, 450] (25), [M^+- $CH_2C_6H_3(OH)_2$-Br, 412] (22), [M^+-$C_2H_4C_6H_3(OH)_2$-CO_2-Br, 355] (98); HR-MS (FAB^+) m/z: 612.0408 (calcd for $C_{24}H_{31}BrNO_5Sn$); observed: 612.0405.

(5*S*)-2,2-Di-*n*-butyl-6-aza-1,3-dioxa-5-(3',4'-dihydroxybenzyl)-12-chloro-2-stannabenzocyclodonone-6,8-dien-4-one (**3g**)

The general procedure with 0.1109 g (0.803 mmol) 5-Chlorosalicylaldehyde resulted in compound **3g** as a yellow powder in 69% yield (0.3141 g); mp 108-111 °C. [α] $^{20}_D$= -197.6

(C=1, Methanol). Molar conductance Λ_M (1×10^{-3} M, methanol): 14.0 ohm^{-1} cm^2 mol^{-1} (non-electrolyte). UV-Vis (Methanol) [λ_{max}/nm (logε/mol L^{-1})$^{-1}$ cm^{-1}]: 205 (22198), π–π* (aromatic), 285 (4616), π–π* (C=N), 400 (1746), n–π* (C=N). IR (KBr, cm^{-1}): 2955 ν(OH $_{alcohol}$), 1647 ν_{sym}(COO$^-$), 1614 ν(C=N), 1378 ν_{asym} (COO$^-$),1258 (C-O $_{arom}$), 578 ν(Sn-C), 543 ν(Sn-O), 448 ν(Sn-N). ^{1}H NMR (300.52 MHz, DMSO-*d*$_6$) δ: 8.83 (s,1H, OH), 8.76 (s,1H, OH), 8.37 (s, $^3J^1H$-^{119}Sn = 45.08 Hz, 1H, H-7), 7.38 (dd, *J* = 9.0, 2.7 Hz, 1H, H-11), 7.31 (d, *J* = 2.7 Hz, H-13), 6.67 (d, *J* = 9.0 Hz, 1H, H-10), 6.57 (d, *J* = 8.0 Hz, 1H, H-5'), 6.50 (d, *J* = 1.4 Hz, 1H, H-2'), 6.26 (dd, *J* = 8.0, 1.4 Hz, 1H, H-6'), 4.28 (t, *J* = 6.0 Hz, 1H, H-5), 3.07 (dd, *J* = 15.0, 6.0 Hz, 2H, H-14), 1.61-0.88 (m, 12H, H-α, β, γ, α', β', γ'), 0.83 (t, *J* = 7.2 Hz, 3H, H-δ), 0.74 (t, *J* = 7.2 Hz, 3H, H-δ'). ^{13}C NMR (75.57 MHz, DMSO-*d*$_6$) δ: 173.4 (C-9), 172.3 (C-4), 167.1 (C-7), 145.3 (C-3'), 144.4 (C-4'), 136.4 (C-10), 134.1 (C-13), 125.8 (C-1'), 123.7 (C-11), 120.8 (C-5'), 119.0 (C-12), 118.1 (C-8), 117.1 (C-2'), 115.4 (C-6'), 68.0 (C-5), 39.8 (C-14), 26.7, 26.6 (C-α, C-α'), 25.9, 25.8 (C-β, C-β'), 22.44, 22.3 (C-γ, C-γ'), 13.6, 13.4 (C-δ, C-δ'). ^{119}Sn NMR (112.07 MHz, DMSO-*d*$_6$) δ: -229.78; ^{119}Sn NMR (112.07 MHz, Chloroform-*d*) δ: -194.90. FAB-MS m/z (%): [(M$^+$+1), 668] (8), [M$^+$-CO_2, 524] (13), [M$^+$-2Bu, 544] (8), [M$^+$-2Bu-CO_2, 410] (20), [M$^+$- $CH_2C_6H_3(OH)_2$-Cl, 412] (28), [M$^+$-$C_2H_4C_6H_3(OH)_2$-CO_2-Cl, 355] (100). HR-MS (FAB$^+$) M/Z: 568.0913 (calcd for $C_{24}H_{30}ClNO_5Sn$); observed: 568.0917.

(5*S*)-2,2-Di-*n*-butyl-6-aza-1,3-dioxa-5-(3',4'-dihydroxybenzyl)-12-nitro-2-stannabenzocyclodonone-6,8-dien-4-one (**3h**)

The general procedure with 0.1109 g (0.803 mmol) 5-Nitrosalicylaldehyde afforded compound **3h** as a yellow powder in 85% yield (0.3917 g); m.p. $_{dec}$ 195 °C. [α] $^{20}_D$= -49.6 (C=1, Methanol). Molar conductance Λ_M (1×10^{-3} M, Methanol): 14.0 ohm^{-1} cm^2 mol^{-1} (non-electrolyte). UV-Vis (Methanol) [λ_{max}/nm (logε/mol L^{-1})$^{-1}$ cm^{-1}]; 205 (40228), π–π* (aromatic), 280 (6774), π–π* (C=N), 340 (8150), n–π* (C=N). IR (KBr, cm^{-1}): 3083 ν(OH $_{alcohol}$), 1615 ν_{asym} (COO$^-$),1596 ν(C=N), 1525 ν_{asym}(O-N=O), 1348 ν_{sym}(COO$^-$), 1262 ν(C-O $_{arom}$), 595 ν(Sn-C), 522 ν(Sn-O), 433 ν(Sn-N); ^{1}H NMR (300.52 MHz, DMSO-*d*$_6$) δ: 9.02 (s, 1H, OH'), 8.82 (s, 1H, OH'), 8.47 (s, $^3J^1H$-^{119}Sn = 33.06 Hz, 1H, H-7), 8.14 (dd, *J* = 9.3, 3.1 Hz, 1H, H-10), 8.04 (d, *J* = 2.8 Hz, 1H, H-13), 6.71 (d, *J* = 9.3 Hz, 1H, H-11), 6.56 (d, *J* =

8.0 Hz, 1H, H-6'), 6.51 (d, *J* = 1.7 Hz, 1H, H-2'), 6.29 (dd, *J* = 8.0, 1.8 Hz, 1H, H-5'), 4.31 (t, *J* = 5.5 Hz, 1H, H-5), 3.09 (dd, *J* = 13.8, 5.6 Hz, 2H, H-14), 1.74 – 0.91 (m, 12H, Hα, β, γ, α', β', γ'), 0.82 (t, *J* = 7.1 Hz, 3H, H-δ'), 0.73 (t, *J* = 7.2 Hz, 3H, H-δ). ^{13}C NMR (75.57 MHz, DMSO-d_6) δ: 173.55 (C-9), 173.07 (C-4), 172.45 (C-7), 145.34 (C-3'), 144.46 (C-4'), 136.07 (C-12), 133.43 (C-13), 130.60 (C-10), 125.92 (C-1'), 122.72 (C-11), 120.79 (C-5'), 117.20 (C-2'), 116.62 (C-8), 115.36 (C-6'), 68.47 (C-5), 39.15 (C-14), 26.73, 26.64 (C-α', C-α), 25.93, 25.77 (C-β', C-β), 24.99, 24.83 (C-γ', C-γ), 13.59, 13.44 (C-δ', C-δ). ^{119}Sn NMR (112.07 MHz, DMSO-d_6) δ: -196.3; ^{119}Sn NMR (112.07 MHz, Chloroform-*d*) δ: -198.0; FAB-MS m/z (%): [(M^++1), 579] (8), [(M^+-Bu), 522] (6), [M^+- CO_2, 524] (13), [M^+-2Bu, 465] (5), [M^+-NO_2-CO_2, 489] (9), [M^+- $CH_2C_6H_3(OH)_2$, 456] (10). HR-MS (FAB^+) M/Z: 579.1153 (calcd for ($C_{24}H_{31}N_2O_7Sn$); observed: 579.1150.

2.4 Cytotoxic Activity Assay

The cytotoxic activity of the compounds (and cisplatin as the reference) was evaluated by the sulforhodamine B assay [29, 30], carried out on the following human cancer cell lines: U-251 (glioblastoma), K-562 (chronic myelogenous *leukemia*), HCT-15 (colorectal), MCF-7 (breast), MB-231 (breast) and SKLU-1 *(*non-*small cell* lung).

2.5 Solubility and stability

All the complexes were soluble in methanol, ethanol and dimethyl sulfoxide, and some of them, showed partial solubility in dichloromethane and chloroform. To examine the biological activity of the complexes and their stability under physiological conditions UV-vis spectra were obtained in different solutions. The first solution used was DMSO-Artificial Seawater (1:1 v/v) and the second solution used was DMSO-DPBS (1:1 v/v), after 24h and 72 h respectively, the UV-vis spectra do not show significant shift of the absorption bands or appearance of any new peaks. In both cases the UV-vis spectra confirmed that the complexes under physiological condition are not degraded. Additionally, in the ^{1}H and ^{119}Sn NMR in DMSO after 48 no-decomposed products or changes in the coordination number were observed.

2.6 In *Vitro* toxicity Bioassay (*Artemia salina*)

The toxicity of all complexes was measured by the brine shrimp lethality test. Brine shrimp cysts (*Artemia salina*) were hatched in a shallow container filled with artificial seawater (Instant Ocean). Approximately 50 mg of cysts were sprinkled into the large compartment, and the contents darkened while the compartment was exposed to ordinary light and incubated at 20-30 °C [31, 32]. After 2 days, nauplii were collected from the lighted side by means of a pipette. A sample for testing at 20 mM was prepared in DMSO. From this stock solution, aliquots were taken and diluted with deionized water to prepare the desired concentrations. To each well of 96-well microplates were added 0.1 mL of seawater containing 10 larvae and 0.1 mL of test solution. Sample concentrations were tested in triplicate. An equivalent solution of DMSO was used as the negative control. Deionized water (0.1 mL) was examined to corroborate the osmotic stress produced by the inoculum of seawater as the control. After 24 hours, dead larvae were counted in a Nikon inverted microscope (4x). Ethanol (0.1 mL) was added to kill the shrimp and a count was again made for the total larvae per well. The LC_{50} value was estimated by means of the Reed-Muench method [33].

2.7 Microorganisms and compounds

The *Candida* strains presently tested were *C. glabrata* CBS138, *C. glabrata* 43, C. *albicans* ATCC 10235 and *C. albicans* 30. *Candida* spp. were stored at -70 °C in cryotubes containing 50% glycerol. All strains of *Candida* were previously incubated in YPD medium (1% yeast extract, 2% casein peptone and 2% dextrose) to corroborate their purity. All compounds used in the current study (including the reference compound, fluconazole) were prepared according to CLSI document M44-A for yeasts [34].

2.8 Susceptibility of *Candida* spp. to the tin compounds

To evaluate the susceptibility of *C. glabrata* and *C. albicans* to organotin compounds, the disk diffusion method was carried out as described in the CLSI, with some modifications [34]. Two layers of Mueller Hinton agar medium (MHA) (meat infusion 0.3%, casein peptone 1.75%, starch 0.15% and 1.5% agar) supplemented with 2% dextrose and 0.5 µg/ml

methylene blue (pH 7.2-7.4) were placed in 100x15 mm petri plates. At first a layer of 15 ml was deposited and left to solidify. Then penicilindros were placed on the MHA and the second layer was added and adjusted by adding cells of *C. glabrata* and *C. albicans* to an OD_{530nm}=0.5. Once the second layer had solidified, an equivalent amount of compound at different concentrations was added to each orifice. The plates were incubated at 30 °C for 16 hours. The assays were performed in triplicate. The DMSO solvent (used to dissolve the compounds) was tested alone as a control to discard any possible inhibitory effect.

2.9 Docking studies

The Protein-ligand interaction was simulated by using molecular docking software Autodock version 4.0.[35] The structure of the ligands were sketched in editor chemical MedChem Designer 3.0 (http://www.simulations-plus.com/software/medchem-designer) and converted in mol^2 in the Open Babel GUI program. [36] The crystal structure of human DNA topoisomerase I (70 Kda) in complex with a 22 Base pair DNA Duplex (PDB:1sc7) was downloaded from the protein data bank (http://www.rcsb.org./pdb). For the preparation of docking, the following parameters were estimated in AutoDock Tools (ADT) [35]: grid dimensions of 90 x 90 x 90 $Å^3$ with points separated by 0.350 Å, and a grid center of X= 85.385, Y= -10.629 and Z= 10.945. Random starting positions, orientations and torsion were established for all ligands. Default values of translation, quaternation and torsion steps were used for the simulation. The hybrid Lamarckian Genetic Algorithm was applied for minimization, also with default parameters. The number of docking runs was 100, considering the docked model with the lowest binding energy for all further studies. The results of docking were analyzed in AutodockTools and edited in Discovery 4.0 Client [37].

3. RESULTS AND DISCUSSION

3.1 Synthesis

The organotin (IV) complexes **3a-3h** were synthesized with a one-pot strategy (Scheme 1). Thus, 3,4-dihydroxi-L-phenylalanine (L-DOPA), the corresponding 5-R-salicylaldehyde (R= H, CH_3, OH, OCH_3, Cl, Br, I, NO_2) and dibutyltin oxide were reacted in a 1:1:1 molar ratio to afford the complexes in yields ranging from 56 to 84%. All the complexes were

soluble in DMSO and methanol, having low conductivity in the latter (in the range of 4 to 14 Ω^{-1} cm^2 mol^{-1}), indicating a non-electrolytic nature.

3.2 Electronic Absorption Spectra

The UV–Vis absorption spectra of complexes **3a-3h**, recorded in a dry methanol solution, exhibited two bands associated with the aromatic ring (π–π*) charge transfer transitions in the range of 205-209 nm and 240-249 nm. The azomethine C═N group showed two bands in the range of 280-290 and 395–409 nm, which could be due to the π–π* and n–π* transitions of the chromophore (C═N), respectively. The dπ–pπ transition, caused by the charge transfer and bonds between the oxygen and nitrogen of the ligands and the vacant 5d orbitals of tin were not observed.

3.3 FT-IR

The analysis of the FT-IR spectra revealed broad stretching OH bands at around 3156-2955 cm^{-1}, attributable to the phenolic bands of the aromatic ring from the L-DOPA moiety. However, the absence of carboxylic acid and the presence of strong bands at 1252–1262 cm^{-1}, corresponding to ν(C─O─phenolate), reflects the deprotonation of the ligand and the formation of a Sn-O bond. The spectra of complexes **3a-h** displayed two different absorption bands in the range of 1615-1652 cm^{-1} and 1348-1375 cm^{-1} (Table 1), which correspond to the ν_{sym}(COO) and ν_{asym}(COO) vibrational modes of the carboxyl groups, respectively. Deacon has proposed that the energy difference between the asymmetric and symmetric carboxylate stretching vibrations $\Delta\nu > 200$ cm^{-1} are associated with an unidentate coordination (Table 1) [38]. Involvement of nitrogen in the coordination was supported by the appearance of the bands corresponding to ν(C=N) and ν(Sn-N) in the regions 1596-1614 and 433-448 cm^{-1}, which confirms coordination through the azomethine nitrogen to the organotin moiety. Additionally, bands at 552-595 and 510-535 cm^{-1} were assigned to ν(Sn-C) and ν(Sn-O), respectively, the observed wavelengths band ranges for the complexes can be explained by the strengths of the bond involved and the mass of the component atoms, additionally, the electronegativity of halogen substituents, have an impact on the spectrum of neighboring group frequencies. In this case, all the absorption bands described above for complexes are consistent with those detected in a number of organotion (IV) derivatives [39, 40]

3.4 Mass Spectra

The molecular species were established by mass spectrometry. The spectra showed the expected peaks for the molecular ions M^++1. In the first stage, the butyl group was lost to form the [M^+ -2Bu] ion. Also detected were the fragment ions [M^+ -2Bu] and [M^+- 2Bu - CH_2-C_6H_3-$(OH)_2$], corresponding to the base peak. For all complexes, there was a similar fragmentation pattern with a characteristic profile in which ^{120}Sn is the most abundant isotope.

3.5 NMR Spectroscopy

The evidence that the pentacoordinated tin heterocyclic ring species had formed was provided by ^{119}Sn, ^{1}H, and ^{13}C NMR spectroscopy. According to the data in literature, the region of ^{119}Sn NMR chemical shifts defines the coordination number of the tin atom. For diorganotin(IV) carboxylate complexes, values in the range of -90 to -190 ppm and -210 to -400 pm are linked to five and six-coordinated complexes, respectively [41]. For complexes **3a**–**3h**, the values are summarized in Table 2. Typical signals attributable to hexacoordinate tin atoms, in the range of -198 to -229 ppm, were observed in the ^{119}Sn NMR spectra when DMSO-*d6* was used. This is a consequence of the coordination of the nitrogen atom to the metal center and the formation of Sn-O bonds. The coordinated character of DMSO could explain the filling of the sixth coordination site. For comparison purpose, therefore, the ^{119}Sn NMR for all complexes was obtained in chloroform. The resulting chemical shifts were found in the range of -192- to -198, as is expected for pentacoordinated complexes (Table 2). In the case of complex **3h,** no significant change was detected in the chemical shift when comparing the spectra of the two solvents, indicating that the coordinative solvent did not influence the coordination number. Additionally, the chemical shifts for **3a**-**3h** are lower than those described for hexacoordinated tin compounds derived from phenylalanine, isoleucine and glycine [21].

The ^{1}H NMR for complexes **3a**–**3h** showed signals in the range of 0.73-1.74 ppm, attributable to the butyl groups bonded to the tin atom, and two triple signals in the range of 0.73-0.83 ppm corresponding to the methyl groups bonded to the butyl groups (due to the asymmetry of the molecule). For the azomethine proton, there was a single signal between 8.21 and 8.47

ppm and characteristic satellites due to ^{3}J (^{1}H-^{119}Sn/^{1}H-^{117}Sn) coupling. The *J* values were in the range of 33-51 Hz, in agreement with previous reports.[40)]

The ^{13}C NMR spectra for **3a**-**3h** revealed two signals in the aliphatic region from 13.1-26.8 ppm, implying the presence of the butyl groups. As evidenced in the ^{1}H NMR, the methylene and methyne groups from the L-DOPA moiety were represented by bands from 67.7-68.4 and 39.2-40.4 ppm, respectively. In the aromatic region, signals for both aromatic rings were identified. The azomethine carbon appeared from 163.5-172 ppm, and the carbonyl group produced chemical shifts in the range from 173.1-174.2 ppm. Unfortunately, and despite all efforts, the satellite signals due to ^{119}/^{117}Sn-^{13}C coupling could not be perceived in the ^{13}C NMR data.

3.6 Cytotoxicity and Structure-Activity Relationship (SAR)

An *in vitro* determination was made of the effect of all the synthesized complexes on the growth human cancer cell lines: U-251 (glioblastoma), K-562 (chronic myelogenous leukemia), HCT-15 (colorectal), MCF-7 (breast), MDA-MB-231(breast) and SKLU-1 *(*non-small cell lung). The sulforhodamine B (SRB) cytotoxicity assay was performed for this purpose. All compounds exhibited an inhibitory effect against all the tumor cells. The complexes share the common amino acid (L-DOPA) and phenolate moiety; the main structural differences are the substitution of the aromatic ring with substituents that possess different electronic character. The results were analyzed by means of cell inhibition curves and expressed as IC_{50} values ranging from 0.11 to 2.7μM (for the IC_{50} values, see Table 3). The complexes **3a**-**3h** were substantially more cytotoxic than cisplatin and significantly more effective than topotecan in inhibiting the growth of leukemia, breast and lung cancer cell lines, which were used as positive controls. An analysis of the substituents on the aromatic ring indicates that the presence of electron-donating groups **3a** (MeO), **3b** (OH) and **3c** (CH_3), increase the activity against the tested cell lines while, the opposite effect was observed for the electron withdrawing substituent **3h** (NO_2). Meanwhile, complex **3d** (H) with no substituent on the aromatic ring showed the lower inhibitory effect.

Furthermore, it was generally observed that the presence of the halogenated substituents **3f** (Br) or **3g** (Cl) on the aromatic ring produce an improvement on the activity in comparison to Iodine **3e**(I).

For the two breast cancer cell lines, MCF-7 and MDA-MB231, the IC_{50} values were lower for the latter cells, indicating a higher selectivity on these cells.
The results suggest that the nature of the substituents on the aromatic ring could possibly be associated with the specificity of growth inhibition of tumor cells.

3.7 Toxicity

Multiple biological models are employed for toxicity evaluations. In vitro techniques, such as cell culture systems, are often preferred because of the cost and time. However, direct translation to whole organisms is often difficult to infer. Taking this in mind, we decided to evaluate the toxicity of the synthetized organotin (IV) complexes **3a-3h** not only using a cell culture but also, an *in vivo* biological model with the aim to make a comparative analysis of the results from both assays. For this purpose, a brine shrimp lethality assay was carried out, this biological model is widely used due to the easy accessibility of naupilii hatched from cysts, rapid hatching, and feasibility of handing under laboratory conditions.
For complexes **3a-3h** the median lethal concentration (LC_{50}) was determined (Table 4). Accordingly, the least toxic complex was **3d** (H), which also demonstrated the lowest cytotoxicity towards the cancer cell lines evaluated. In contrast, the highest toxicity was produced by **3e** (I). The complexes **3a-3c** and **3f-3h** were all less toxic than the iodine derivative. Among the halogenated derivatives, the bromine derivative showed the lowest toxic effect on brine shrimp and the highest cytotoxic effect on MDA-MB-231 cell line. For HCT-15, a correlation between toxicity and the cytotoxic effect was observed. However, for U251, K562, MCF-7, MDA-MB-251 and SKLU, the level of toxicity on brine shrimp did not predict the cytotoxic.

3.8 Antifungal activity

The organotin(IV) compounds were evaluated on two strains of *C. glabrata* and two of *C. albicans*, finding that all the test complexes induced antifungal activity against the *Candida* species herein examined. There was a much lower MIC value found for all the organotin(IV) compounds (**3a-3h**) than for fluconazole, the reference drug (Table 5). The MIC values

indicated a very similar antifungal activity by all the test compounds, suggesting that the distinct nature of the substituents bonded to the aromatic ring does not lead to selectivity against the strains evaluated. In accordance with the experimental results, on the other hand, complexes **3a**-**3h** were more active against *C. albicans* than the previously reported organotin(IV) complexes derived from thiosemicarbazones[42]. The organotin (IV) compounds tested presently can be considered as candidates for antifungal agents against *Candida* spp.

3.9 Molecular docking

A molecular docking study was carried out to predict the binding mode of the organotin (IV) compounds at the active site of the DNA topoisomerase enzyme. DNA topoisomerase has been used as a therapeutic target in the search of new anticancer agents [43], and topotecan (an inhibitor of topoisomerase I) as the control. The latter compound has been extensively studied and administered in anticancer therapy [44]. The current results reveal that an organic moiety of the organotin(IV) complexes bind to important amino acids side chains of the topoisomerase I enzyme (e.g., Ile535, Arg364 and Asp533), to which the reference compound (topotecan) also binds, in no case metallic-topisomerase I interaction was observed.

The organotin(IV) compounds displayed hydrophilic, hydrophobic and pi-cation-anion interactions with these amino acids (Figures 1a-1j). Most of the organotin(IV) derivatives exhibited a hydrophobic interaction between residue Arg364 and the benzene ring of catechol. Topotecan and compound **3a** share an interaction with residue Asp533. Evaluation was also made of the interaction between the test complexes and the DNA structure, finding that they interact with some of the same DNA regions as topotecan (e.g., DA113, DC112 and DT10).

The evidence of a comparable binding mode coincides with the identical binding energy values obtained for compound **3a** and topotecan (-9.20 and -9.21, respectively). Compound **3a** is an organotin(IV) derivative and one of the most active against the growth of the human

cancer cell lines herein evaluated. According to the docking studies (Table 6) and the results of cytotoxic activity, the binding energies of the test compounds are similar to the value detected for topotecan and substantially better than the -4.0 value for *cis*-platin. Whereas inhibition of DNA synthesis is the mechanism reported for *cis*-platin [45]. Derivatives **3a**, **3f** and **3b** had the best binding energies and had the greatest activity in most of the cell lines. These observations coincide with the idea that in their binding mode, the newly synthesized complexes and topotecan share affinity for certain amino acid residues at the active site of the topoisomerase enzyme I, and also have DNA regions in common. Therefore, the current results suggest that the test organotin(IV) compounds could possibly be an alternative for anticancer therapy. Other studies have proposed organotin(IV) compounds as anticancer agents as well [46].

CONCLUSIONS

The one-pot reaction proved to be an excellent strategy for the synthesis of organotin(IV) complexes, which were isolated in good yields. The level of toxicity found in the brine shrimp lethality assay showed no correlation with the cytotoxic effect of the test compounds on the U251, K562, MCF-7, MDA-MB-251 and SKLU-1 cancer cell lines, indicating that in vitro studies of the biological activity of cytotoxic compounds may not predict in vivo toxicity. The organotin(IV) complexes exhibited pronounced inhibitory activity against the growth of the six human cancer cell lines tested. The potency of the cytotoxic activity against the cancer cell lines depended on the nature of the substituent bonded to the aromatic ring. We modify the substitution of the aromatic ring with electron-donating and electron-withdrawing substituents on the aromatic ring and carried out a cytotoxic test on cancer cell lines to stablish the possible structure activity for this system, in general the best analogues with the lower CI_{50} value were the electron-donating groups **3a** (MeO), **3b** (OH), **3c** (CH_3) in the five position on aromatic ring, the halo substituents bromine and chloride also have favorable cytotoxic activity; for all evaluated cell lines **3f** (Br) had equal or better activity than **3g** (Cl). The docking studies indicate that the binding mode of the organotin(IV) complexes is comparable to that of topotecan and better than *cis*platin, these results are in agreement with the cytotoxic activity assay. Additionally, the *in silico* prediction showed a remarkable inhibitory effect for complexes **3a** (OCH_3) and **3f** (Br). The test compounds have affinity for

some of the same amino acid side chains (Ile535, Arg364 and Asp533) and DNA regions (DA113, DC112 and DT10).

Consequently, these compounds are possible candidates for anticancer therapy due to their high cytotoxic effect. The susceptibility of *C. glabrata* and *C. albicans* to these compounds points to the importance of further research on their antifungal activity. The current findings open new possibilities for the design of organometallic derivatives with diverse pharmacological activities.

CONFLICT OF INTEREST

The authors declare no conflict of interest.

ACKNOWLEDGEMENTS

The authors wish to thank PAPIIT IN204417 for financial assistance, and María de la Paz Orta, María del Carmen García, Luis Velasco and Javier Pérez for IR spectroscopy and mass spectrometry technical support. Erika Rocha is grateful to CONACyT for the MS fellowship.

REFERENCES

1) Kajal A., Bala S., Sharma N., Kamboj S., Saini V. *International Journal of Medicinal Chemistry*, **2014**, 11 (2014).
2) Sondhi S. M., Singh N., Kumar A., Lozach O., Meijer L. *Bioorg. Med. Chem.,* **14**, 3758-3765 (2006).
3) Krátký M., Dzurková M., Janoušek J., Konečná K., Trejtnar F., Stolaříková J., Vinšová J. *Molecules,* **22**, 1573 (2017).
4) Devi J., Devi S., Kumar A. *Med. Chem. Comm.,* **7**, 932-947 (2016).
5) Aly M. M., Mohamed Y. A., El-Bayouki K. A. M., Basyouni W. M., Abbas S. Y. *Eur. J. Med. Chem.,* **45**, 3365-3373 (2010).
6) Ahmad M., Perveen Z., Bortoluzzi A. J., Hameed S., Shah M. R., Tariq M., ud Din G., Anwar M. *J. Struct. Chem.,* **58**, 297-303 (2017).
7) Panneerselvam P., Nair R. R., Vijayalakshmi G., Subramanian E. H., Sridhar S. K. *Eur. J. Med. Chem.*, **40**, 225-229 (2005).
8) Dao V.-T., Dowd M. K., Martin M.-T., Gaspard C., Mayer M., Michelot R. J. *Eur. J. Med. Chem.,* **39**, 619-624 (2004).
9) Al Zoubi W., Al-Hamdani A. A. S., Kaseem M. *Appl. Organomet. Chem.,* **30**, 810-817 (2016).

10) Prabhakara C. T., Patil S. A., Kulkarni A. D., Naik V. H., Manjunatha M., Kinnal S. M., Badami P. S. *J. Photochem. Phobiol. B.,* **148**, 322-332 (2015).
11) Khan K. M., Khan M., Ali M., Taha M., Rasheed S., Perveen S., Choudhary M. I. *Bioorg. Med. Chem.*, **17**, 7795-7801 (2009).
12) Thomas A. B., Nanda R. K., Kothapalli L. P., Hamane S. C. *Arab. J. Chem.,* **9**, S79-S90 (2016).
13) Li W., Zhang Z.-W., Ren S.-M., Sibiril Y., Parent Massin D., Jiang T. *Chem. Biol. Drug. Des.,* **73**, 682-686 (2009).
14) Hussain M., Ahmad M. S., Siddique A., Hanif M., Ali S., Mirza B. *Chem. Biol. Drug. Des.,* **74**, 183−189 (2009).
15) Prabhakaran R., Krishnan V., Pasumpon K., Sukanya D., Wendel E., Jayabalakrishnan C., Bertagnolli H., Natarajan K. *Appl. Organomet. Chem.,* **20**, 203-213 (2006).
16) Singh H. L., Varshney A. K. *Appl. Organomet. Chem.*, **15**, 762-768 (2001).
17) Souba W. W., Pacitti A. J. *J. Parenter. Enteral. Nutr.*, **16**, 569-578 (1992).
18) Fahn S. *J. Neural Transm. Suppl.*, **71**, 1-15 (2006).
19) Hernández-Altamirano R., Mena-Cervantes V. Y., Chávez-Miyauchi T. E., Nieto-Álvarez D. A., Domínguez-Aguilar M. A., Zamudio-Rivera L. S., Barba V., Fernández-Perrino F. J., Pérez-Miranda S., Beltrán H. I. *Polyhedron,* **52**, 301-307 (2013).
20) Basu Baul T. S., Kehie P., Duthie A., Guchhait N., Raviprakash N., Mokhamatam R. B., Manna S. K., Armata N., Scopelliti M., Wang R., Englert U. *J. Inorg. Biochem.*, **168**, 76-89 (2017).
21) Singh H. L., Singh J. *Bioinorganic Chemistry and Applications,* **2014**, 12 (2014).
22) Basu Baul T. S., Masharing C., Ruisi G., Jirásko R., Holčapek M., de Vos D., Wolstenholme D., Linden A. *J. Organomet. Chem.*, **692**, 4849-4862 (2007).
23) Tian L., Sun Y., Qian B., Yang G., Yu Y., Shang Z., Zheng X. *Appl. Organomet. Chem.,* **19**, 1127-1131 (2005).
24) Mala N., Rakesh Y. *Bull. Chem. Soc. Jpn.,* **70**, 1331-1337 (1997).
25) Nath M., Saini P. K. *Dalton Trans.,* **40**, 7077-7121 (2011).
26) Pfaller M. A., Diekema D. J. *Clin. Microbiol. Rev.,* **20**, 133-163 (2007).
27) Pfaller M. A., Diekema D. J. *J. Clin. Microbiol.*, **42**, 4419-4431 (2004).
28) Pasqualotto A. C., Denning D. W. *J. Atimicrob. Chemother.*, **61**, i19-i30 (2008).
29) Monks A., Scudiero D., Skehan P., Shoemaker R., Paull K., Vistica D., Hose C., Langley J., Cronise P., Vaigro-Wolff A., Gray-Goodrich M., Campbell H., Mayo J., Boyd M. *J. Natl. Cancer Inst.,* **83**, 757−766 (1991).
30) Gomez E., Contreras-Ordonez G., Ramirez-Apan T. *Chem Pharm Bull (Tokyo),* **54**, 54-57 (2006).
31) Meyer B. N., Ferrigni N. R., Putnam J. E., Jacobsen L. B., Nichols D. E., McLaughlin J. L. *Planta Med.*, **45**, 31-34 (1982).
32) Solis P. N., Wright C. W., Anderson M. M., Gupta M. P., Phillipson J. D. *Planta Med.*, **59**, 250-252 (1993).
33) Reed L. J., Muench H. *Am. J. Epidemiol.*, **27**, 493-497 (1938).
34) . *Approved standard M44-A Clinical and Laboratory standars Institute, Wayne, Pa.,* **24**, (2004).
35) Morris G. M., Huey R., Lindstrom W., Sanner M. F., Belew R. K., Goodsell D. S., Olson A. J. *J. Comput. Chem.,* **30**, 2785-2791 (2009).

36) O'Boyle N. M., Banck M., James C. A., Morley C., Vandermeersch T., Hutchison G. R. *J. Cheminform.*, **3**, 33 (2011).
37) Dassault Systèmes BIOVIA D. S. M. E., Release 2017, San Diego: Dassault Systèmes, **2016**.
38) Deacon G. B., Phillips R. J. *Coord. Chem. Rev.*, **33**, 227−250 (1980).
39) Gielen M. *Appl. Organomet. Chem.*, **16**, 481-494 (2002).
40) Galván-Hidalgo J. M., Gómez E., Ramírez-Apan T., Nieto-Camacho A., Hernández-Ortega S. *Med Chem Res*, **24**, 3621−3631 (2015).
41) Holeček J., Nádvorník M., Handlíř K., Lyčka A. *J. Organomet. Chem.*, **315**, 299-308 (1986).
42) Parrilha G. L., da Silva J. G., Gouveia L. F., Gasparoto A. K., Dias R. P., Rocha W. R., Santos D. A., Speziali N. L., Beraldo H. *Eur. J. Med. Chem.*, **46**, 1473-1482 (2011).
43) Singh S., Das T., Awasthi M., Pandey V. P., Pandey B., Dwivedi U. N. Biotechnol. Appl. Biochem., **63**, 125-137 (2016).
44) Mancini G., D'Annessa I., Coletta A., Sanna N., Chillemi G., Desideri A. *Plos One*, **5**, e10934 (2010).
45) Dasari S., Bernard Tchounwou P. *Eur. J. Pharmacol.*, **740**, 364-378 (2014).
46) Tabassum S., Afzal M., Arjmand F. *Eur. J. Med. Chem.*, **74**, 694-702 (2014).

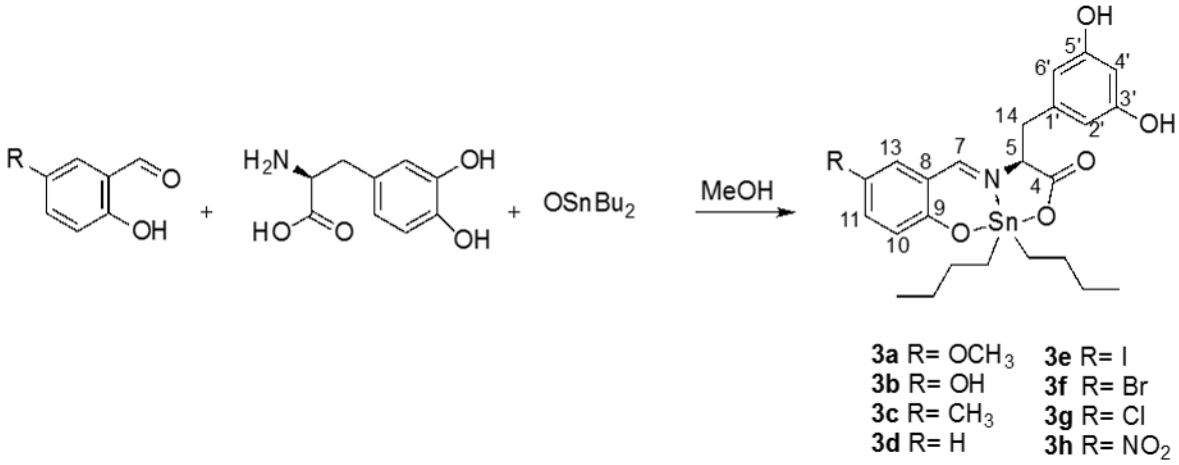

Scheme 1. *Synthesis of* dibutyltin(IV) complexes via one-pot reaction.

Figures

a)

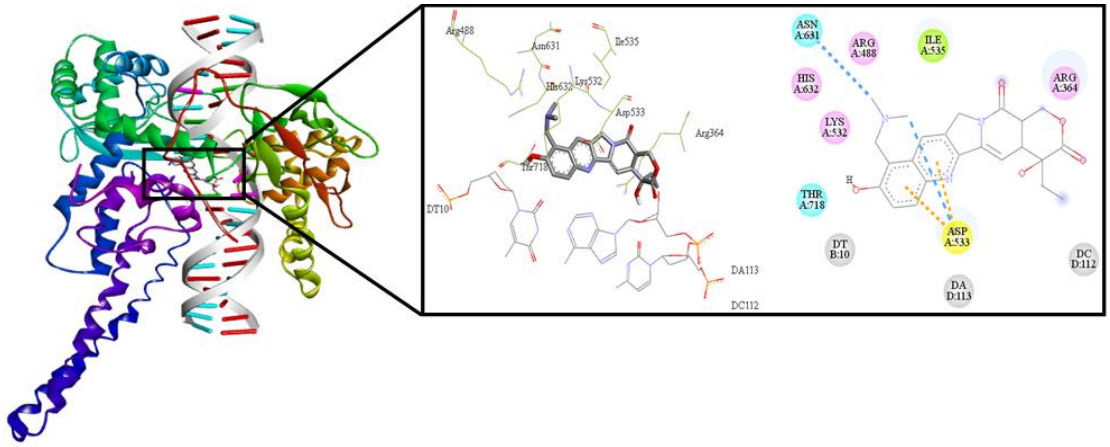
Arg488
Asn631
Ile535
His632
Lys532
Asp533
Arg364
Thr718
DT10
DA113
DC112
ASN A:631
ARG A:488
ILE A:535
HIS A:632
ARG A:364
LYS A:532
THR A:718
ASP A:533
DT B:10
DC D:112
DA D:113

b)

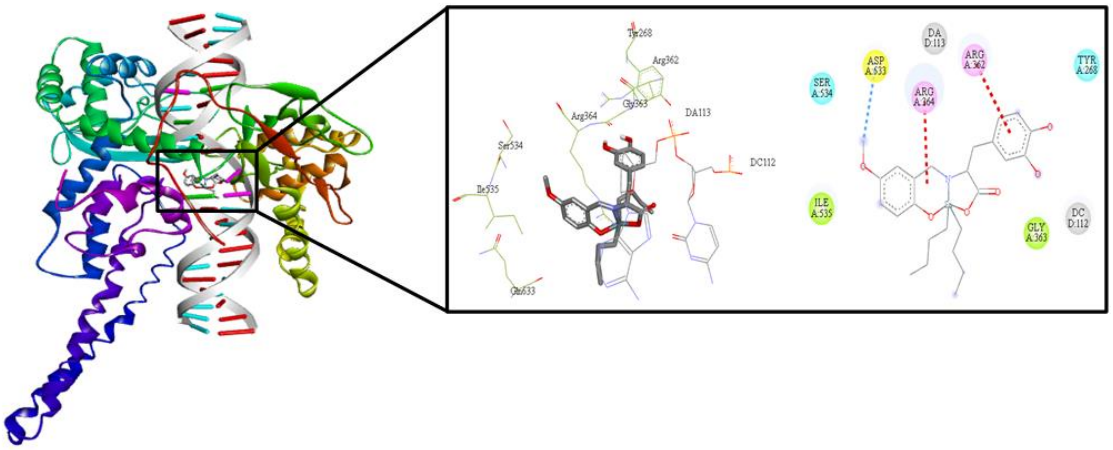
Thr268
Arg362
Gly363
Arg364
DA113
Ser534
Ile535
DC112
Gln633
DA D:113
ASP A:533
ARG A:362
TYR A:268
SER A:534
ARG A:364
ILE A:535
GLY A:363
DC D:112

c)

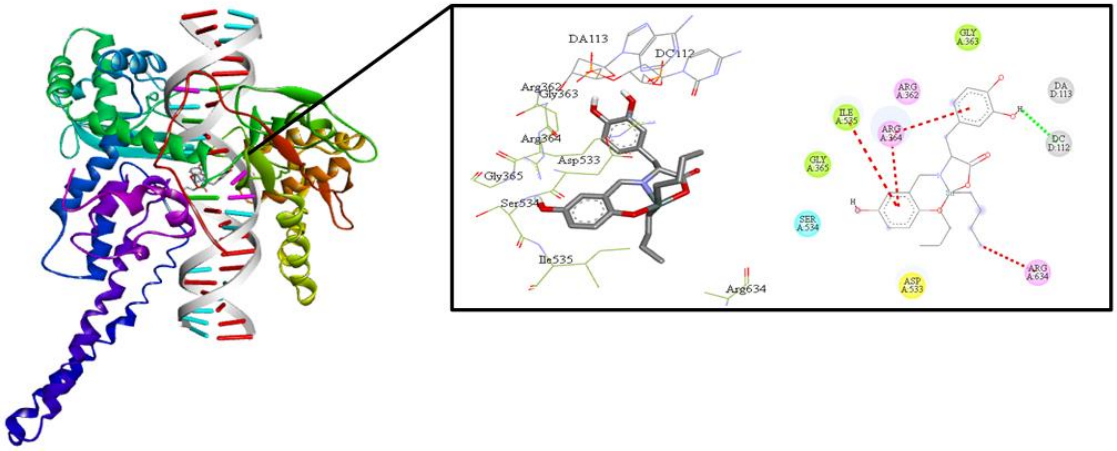
DA113
DC112
Arg362
Gly363
Arg364
Asp533
Gly365
Ser534
Ile535
Arg634
GLY A:363
ARG A:362
DA D:113
ILE A:535
ARG A:364
DC D:112
GLY A:365
SER A:534
ASP A:533
ARG A:634

d)

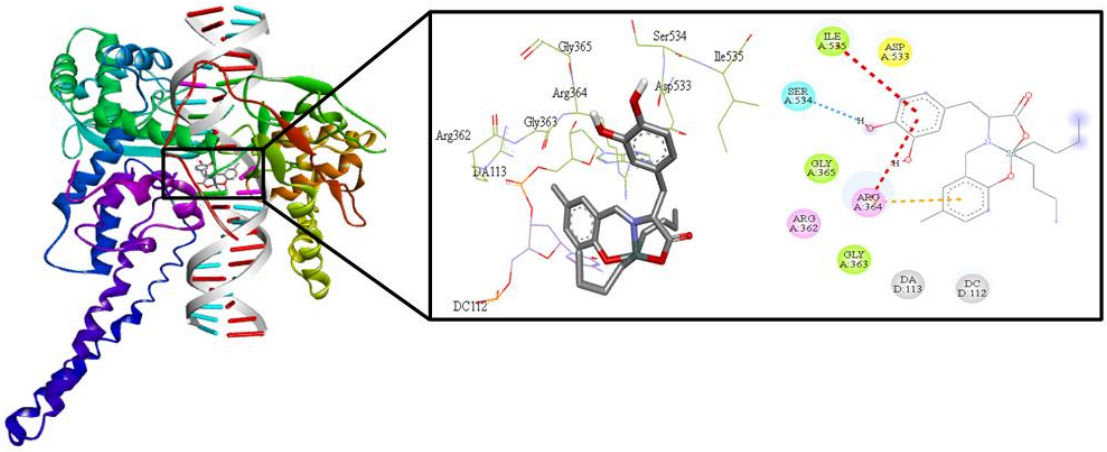
Gly365
Ser534
Ile535
Arg364
Asp533
Arg362
Gly363
DA113
DC112
ILE A.535
ASP A.533
SER A.534
GLY A.365
ARG A.364
ARG A.362
GLY A.363
DA D.113
DC D.112

e)

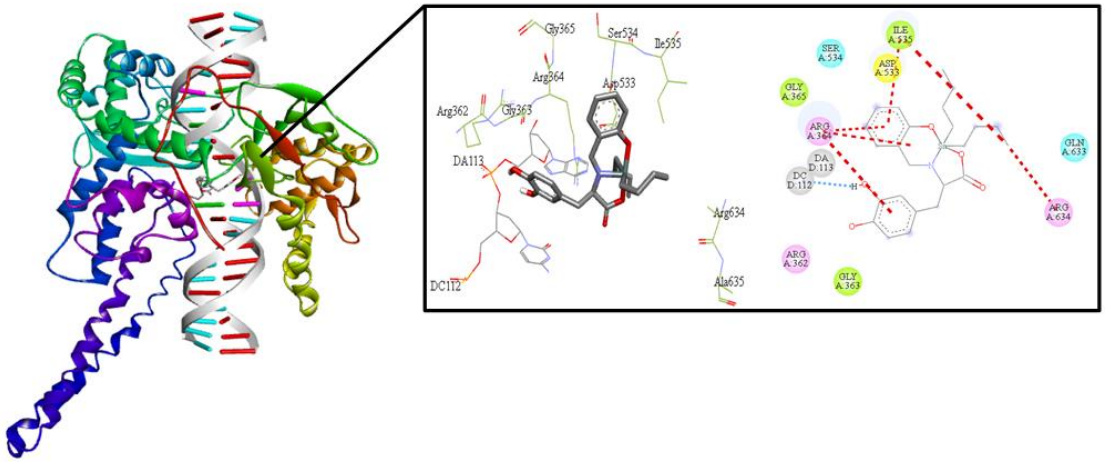
Gly365
Ser524
Ile535
Arg364
Asp533
Arg362
Gly363
DA113
DC112
Arg634
Ala635
ILE A.535
SER A.534
ASP A.533
GLY A.365
ARG A.364
DA D.113
DC D.112
GLN A.633
ARG A.634
ARG A.362
GLY A.363

f)

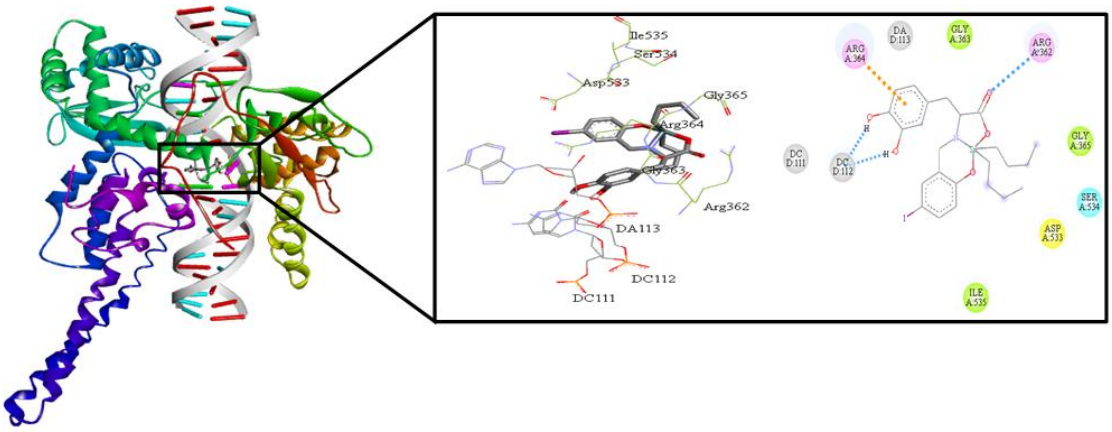
Ile535
Ser534
Asp583
Gly365
Arg364
Gly363
Arg362
DA113
DC112
DC111
ARG A.364
DA D.113
GLY A.363
ARG A.362
DC D.111
DC D.112
GLY A.365
SER A.534
ASP A.533
ILE A.535

g)

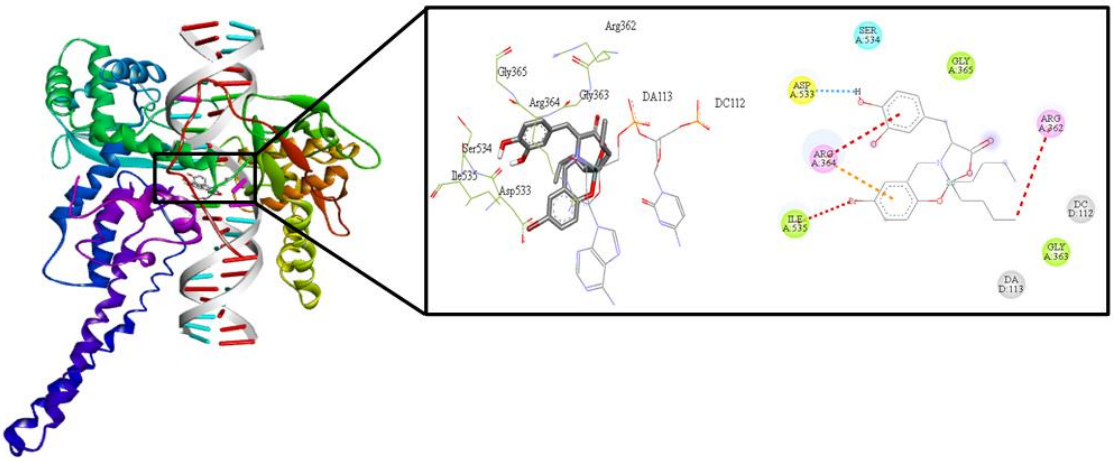
Arg362
Gly365
Arg364
Gly363
DA113
DC112
Ser534
Ile535
Asp533
SER A.534
GLY A.365
ASP A.533
ARG A.362
ARG A.364
ILE A.535
DC D.112
GLY A.363
DA D.113

h)

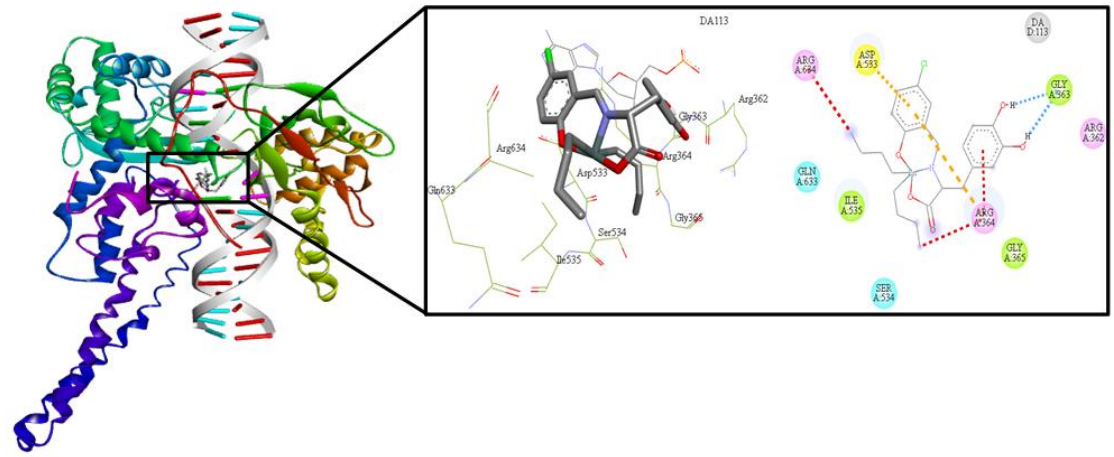
DA113
DA D.113
ARG A.644
ASP A.583
GLY A.963
Arg362
Gly363
ARG A.362
Arg634
Arg364
Asp533
GLN A.633
ILE A.535
Gln633
ARG A.364
Gly365
GLY A.365
Ser534
Ile535
SER A.534

i)

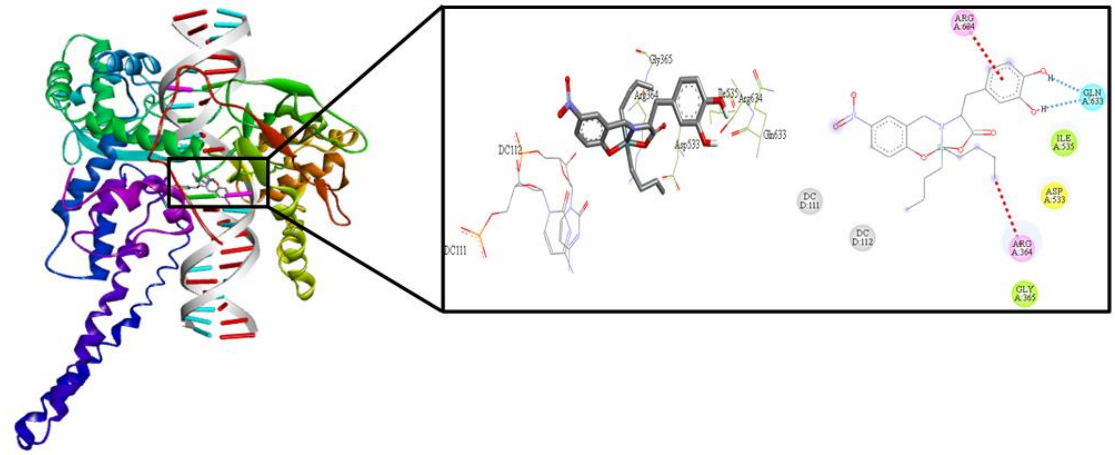
ARG A.644
Gly365
GLN A.633
Asp534
Ile535
Asp533
Gln633
DC112
ILE A.535
DC D.111
ASP A.533
DC D.112
ARG A.364
DC111
GLY A.365

Figures 1a-j. Prediction of the binding mode of tin(IV) complexes at the active site of the DNA Topoisomerase I enzyme. The protein is represented as a flat ribbon and the complex in a stick model: a) Topotecan, b) **3a**, c) **3b**, d) **3c**, e) **3d**, f) **3e**, g) **3f**, h) **3g** and i) **3h**. The compounds are depicted in 3D and 2D, showing their interactions with enzyme residues and DNA regions. In the 2D representation, the dotted lines portray hydrogen bonds (blue) as well as hydrophobic (red) and electrostatic interactions (orange). In cyan blue, the accessible surface of the ligand and residues of the enzyme are illustrated. Polar (cyan blue) and non-polar amino acids (green), acids (yellow), bases (pink) and interactions with the DNA complex (gray) are indicated in circles.

Table 1. Assignment of characteristic FT vibrations (cm^{-1}).

Compound	$\nu_{asym}COO^-$	$\nu_{sym}COO^-$	$\Delta\nu$	$\nu C=N$
3a	1652	1359	293	1598
3b	1628	1375	253	1606
3c	1621	1374	247	1598
3d	1647	1345	302	1609
3e	1645	1375	270	1607
3f	1649	1354	295	1612
3g	1647	1378	269	1614
3h	1615	1348	267	1596

Table 2. ^{119}Sn NMR (112.04 MHz) data for complexes **3a**-**3h**.

Compound	$CDCl_3$	DMSO-d_6
3a	-192.5	-216.8
3b	-193.4	-214.0
3c	-193.9	-218.1
3d	-194.6	-220.8
3e	-195.1	-227.8
3f	-195.0	-229.9
3g	-194.9	-229.8
3h	-198.0	-196.3

Table 3. Inhibitory Concentration $(IC)_{50}$ (μM) for complexes **3a**-**3h**.

Compound	U-251	K-562	HCT-15	MDA-MB231	MCF-7	SKLU-1
3a	0.18±0.022	0.13±0.02	0.90±0.01	0.29±0.01	0.29±0.05	0.27±0.01
3b	0.21±0.005	0.11±0.007	0.86±0.03	0.34±0.07	0.33±0.05	0.33±0.01
3c	0.33±0.007	0.15±0.02	0.95±0.08	0.21±0.04	0.76±0.04	0.26±0.02
3d	0.53±0.01	0.53±0.02	2.7±0.3	1.28±0.06	1.26±0.03	0.76±0.01
3e	0.41±0.01	0.37±0.02	0.72±0.02	0.42±0.03	0.59±0.03	0.42±0.01
3f	0.15±0.019	0.18±0.01	1.12±0.07	0.36±0.03	0.73±0.04	0.37±0.05
3g	0.18±0.007	0.184±0.04	1.12±0.12	0.45±0.009	0.71±0.067	0.5±0.05
3h	0.49±0.02	0.34±0.01	1.0±0.03	0.44±0.01	0.66±0.08	0.47±0.03
Cis-platin	9.09±0.80	15.20±1.40	13.83±0.70	13.03±1.30	13.03±1.30	7.13±0.20
Topotecan	0.03±0.003	0.5±0.07	0.5±0.05	0.473±0.023[46)]	0.1±0.02	2.0±0.1

Data represent the average of three or four independent assays and are expressed as the mean ± standard error (SE)

Table 4. Median lethal centration (LC_{50}) of ***3a-3h*** in the brine shrimp lethality assay.

Compound	CL_{50} μM
3a	34.91 ± 1.40
3b	26.98 ± 1.48
3c	40.92 ± 1.48
3d	68.87 ± 1.27
3e	8.08 ± 1.23
3f	59.57± 1.35
3g	38.64 ± 1.42
3h	43.46 ± 1.37

Table 5. Susceptibility of *Candida* spp. to antifungal agents, evaluated by CLSI-M44-A.

Inhibitor	***C. glabrata*** **CBS138**	***C. glabrata*** **43**	***C. albicans*** **ATCC 10235**	***C. albicans*** **30**
Fluconazole	[μg/ml] MIC ≥80	[μg/ml] MIC ≥1,280	[μg/ml] MIC ≥10	[μg/ml] MIC ≥20
3a-3h	≥3.12	≥3.12	≥3.12	≥3.12

MIC: minimum inhibitory concentration.

Table 6. Results of molecular docking of the tin(IV) complexes on the active site of DNA topoisomerase I.

Compound	Binding energy (Kcal/mol)
Topotecan	-9.21
***Cis*-platin**	-4.0
3a	-9.20
3b	-8.96
3c	-8.87
3d	-8.74
3e	-8.88
3f	-9.19
3g	-7.91
3h	-8.29